


Superuniversality of dimerized $SU(N + M)$ spin chains

A. M. M. Pruisken^{1,*}, Bimla Danu^{2,†} and R. Shankar^{3,‡}

¹*Institute for Theoretical Physics, Science Park 904, 1098 XH Amsterdam, The Netherlands*

²*Institut für Theoretische Physik und Astrophysik and Würzburg-Dresden Cluster of Excellence ct.qmat, Universität Würzburg, 97074 Würzburg, Germany*

³*The Institute of Mathematical Sciences, C I T Campus, Chennai 600 113, India*

 (Received 26 December 2021; revised 13 March 2022; accepted 14 March 2022; published 6 April 2022)

We explore the physics of the quantum Hall effect using the Haldane mapping of dimerized $SU(N + M)$ spin chains, the large N expansion, and the density matrix renormalization group technique. We show that while the transition is first order for $N + M > 2$, the system at zero temperature nevertheless displays a continuously diverging length scale ξ (correlation length). The numerical results for $(N, M) = (3, 1), (2, 2), (5, 1),$ and $(7, 1)$ indicate that ξ is a directly observable physical quantity, namely the spatial width of the edge states. We relate the physical observables of the quantum spin chain to those of the quantum Hall system (and, hence, the ϑ vacuum concept in quantum field theory). Our numerical investigations provide strong evidence for the conjecture of superuniversality which says that the dimerized spin chain quite generally displays all the basic features of the quantum Hall effect, independent of the specific values of N and M . For the cases at hand we show that the singularity structure of the quantum Hall plateau transitions involves a universal function with two scale parameters that may in general depend on N and M . This includes not only the Hall conductance but also the ground state energy as well as the correlation length ξ with varying values of $\vartheta \sim \pi$.

DOI: [10.1103/PhysRevB.105.155111](https://doi.org/10.1103/PhysRevB.105.155111)

I. INTRODUCTION

In this paper we are addressing several long standing issues relating to the robustness of the integer quantum Hall plateaus as well as the concept of superuniversality in the theory of dimerized quantum spin chains. How is the physics of $SU(N + M)$ spin chains, the main focus in this paper, related to the physics of the quantum Hall effect (QHE)? The answer to this question is twofold. First, using replica field theory, Levine, Libby, and Pruisken showed that the physics of the QHE can be inferred from the grassmannian $U(N + M)/U(N) \times U(M)$ sigma models in the presence of the so called ϑ angle [1–5]. While N and M are integers, the physics of the electron gas is recovered in the analytic continuation $N, M \rightarrow 0$ (replica limit). Second, Haldane has shown that the low energy physics of the $SU(2)$ spin chain can be mapped onto that of an $SU(2)/U(1)$ sigma model [6,7]. In this special case with $N, M = 1$ the angle ϑ only takes on the value 0 or π depending on whether the spin S is an even or odd multiple of $\frac{1}{2}$. In later work [8] it was argued that the mapping can be generalized to include $SU(N + M)$ spin chains with a dimerization parameter which we term ε . This leads to the same grassmannian sigma model with a parameter ϑ that varies continuously with varying values of ε .

The above derivations [6–8] are valid in the $S \rightarrow \infty$ limit. However, they have technical problems that complicate a sys-

tematic $1/S$ expansion of the parameters of the field theory. An alternative derivation detailed in Ref. [9] resolves these problems for the $SU(1 + 1)$ case and formulates a well defined $1/S$ expansion. These results are easily generalized to the $SU(N + M)$ case and will be presented in a forthcoming publication [10].

It is well known that the sigma model flows toward the strong coupling regime [3,11] which is, generally speaking, inaccessible analytically. However, it is also well known that this regime is numerically accessible, namely based on the density matrix renormalization group (DMRG) approach to quantum spin chains [12,13]. The main purpose of the present paper, therefore, is to use the DMRG as an unequivocal test of the distinctly different strong coupling ideas that over the years have emerged in the study of both $SU(N + M)$ quantum spin chains [9,14] and the closely related grassmannian $U(N + M)/U(N) \times U(M)$ sigma model [4,15].

Quite surprisingly, the fundamental significance of the “massless chiral edge excitations” in the problem of the QHE or equivalently, the “dangling edge spins” in the quantum spin chain, has not been fully appreciated so far. These edge excitations are important not only in the definition of the transport coefficients (“conductances” [9,14,16,17]) but also in our conceptual understanding of more general issues in quantum field theory, notably the quantization of topological charge, the existence of robust topological quantum numbers, etc. [4,18].

Advances along these lines have ultimately led to the resolution of old controversies that have spanned the subject to date. We mention, in particular, the “large N ” picture of the ϑ

* a.m.m.pruisken@contact.uva.nl

† bimla.danu@physik.uni-wuerzburg.de

‡ shankar@imsc.res.in

vacuum concept [19–23] as opposed to the distinctly different “instanton” picture [24–26]. However, these different views have in fact turned out to be complementary [4,15]. This new development is consistent with the original critique by Jevicki [27] and is diametrically opposite to what historically has been dubbed “the arena of bloody controversies” [28].

It is clear that the conflicting views in quantum field theory have had a dramatic impact on the development of a microscopic theory of the quantum Hall effect. Besides the *robust quantization* which emerged as a new and unexpected feature of the ϑ angle, the idea of a *continuously diverging* correlation length ξ —describing the quantum Hall plateau transition—has been a particularly difficult stumbling block for many years [29–31]. These otherwise well established experimental phenomena were believed to be “incompatible” [29,30,32] with the general views based on the large N picture which indicated, amongst many other things, that the transition at $\vartheta = \pi$ is a *first order* one, for all values $N + M > 2$. Such beliefs have, in turn, set the stage for incorrect mathematical claims and ideas in the literature such as the “failure” of the replica method, the “superiority” of supersymmetric representations, etc. [32–34].

More recently the large N steepest descend methodology of the CP^{N-1} model has been revisited [4,15]. Unlike the prevailing expectations in the field, it was shown that the physics of the QHE is, in fact, displayed by the ϑ vacuum concept in general, for all non-negative values of N and M . This naturally leads to the idea of *superuniversality* of topological principles which means that mathematical issues such as the replica limit only play a role of secondary significance.

In what follows we shall further explore and extend the superuniversality concept based on the DMRG simulations of the *open* spin chain with an *odd* number of spins and finite N and M . We use the phrase *open* to indicate that the spin chain has physical *edges* (free boundary conditions). Also, dimerized systems with an *odd* number of spins are very useful in demonstrating the physics of the QHE, as detailed in Refs. [9,14].

The numerical data for the ground state energy with varying system size or length (L) and dimerization (ε) are being compared with the large N approach to spin chains [35,36] as well as grassmannian sigma models [4,15]. The DMRG results now serve as a direct check on the general expectation in the field which says that the transition at $\varepsilon = 0$ (or $\vartheta = \pi$) is a first order one, for $N + M > 2$.

The primary focus of this paper, however, is on the physics of the “edge” the details of which are difficult to obtain analytically. We are specifically interested in the magnetic properties of spin chains since they can be used as a probe for the “massless chiral edge excitations” in the problem [16,17,37,38] or, equivalently, the “dangling edge spins” [9,14]. The DMRG data now indicate that the spatial width or “penetration depth” of the edge excitations diverges continuously as ε approaches the critical value (or, equivalently, as the angle ϑ approaches π). This directly measurable physical quantity is naturally identified with the correlation length ξ of the system.

Next, there is the problem of extracting the most fundamental quantity from DMRG, namely the Hall conductance σ_H with varying L and ε . Generally speaking, this kind of computation is complicated since it demands an explicit



FIG. 1. Interacting dimerized spin chain.

knowledge of the “bulk” excitations and those of the “edges” [4,39]. However, by making use of the dual symmetry of the spin chain, along with the macroscopic conservation law for the magnetization, one can introduce an alternative definition of the linear response formula that is suitable for DMRG purposes. This permits a numerical study of the robustness of the QHE as well as the critical singularities of the quantum Hall plateau transition.

In the last part of this paper we propose an extended version of the superuniversality concept that includes the critical behavior of not only the Hall conductance but also the ground state energy as well as the correlation length. After a simple rescaling of the numerical data with $N + M > 2$ we find that the singularity structure can be expressed in terms of a single universal function $F(X)$ where X generally denotes the linear dimension of the system, i.e. it stands for either L or ξ .

II. DIMER MODEL

Introducing a dimerization parameter ε defined by assigning couplings $J(1 + \varepsilon)$ and $J(1 - \varepsilon)$ to adjacent spin pairs (see Fig. 1), we can write the Hamiltonian of the $SU(N + M)$ spin chain as follows:

$$\mathcal{H} = J \sum_j \sum_{\alpha, \beta=1}^{N+M} \{(1 + (-1)^j \varepsilon) \hat{\mathbf{S}}_{j, \alpha \beta} \cdot \hat{\mathbf{S}}_{j+1, \beta \alpha}\}. \quad (1)$$

Here the spin operators satisfy the commutation relation $[\hat{\mathbf{S}}_{\alpha \beta}, \hat{\mathbf{S}}_{\mu \nu}] = \delta_{\mu \beta} \hat{\mathbf{S}}_{\alpha \nu} - \delta_{\alpha \nu} \hat{\mathbf{S}}_{\mu \beta}$. They are in the spin-1/2 representation of $SU(N + M)$ with the little group $U(N) \times U(M)$.

Our main focus is on the open spin chain with edges. This displays an obvious *dual symmetry* $\varepsilon \leftrightarrow -\varepsilon$, provided the total number of sites is odd, say $2N_s + 1$. The effective action of this system is quite simple in the limit where M is finite and $N \rightarrow \infty$ or vice versa. For example, the ground state involves N_s disconnected *dimers* with a total energy

$$E_0(\varepsilon) = -N_s e_2 (1 + |\varepsilon|), \quad (2)$$

where e_2 is the dimer energy for coupling J [35,36]. This result is precisely the same for a *closed* system with $2N_s$ sites, indicating that a *first order* quantum phase transition takes place when the parameter ε goes through zero. The sole difference, however, is that a dangling spin appears at the edge of an open chain. The effective action now involves the solid angle $\Omega[V]$ of the $SU(N + M)$ matrix variable V ,

$$\Omega[V] = \int_0^\beta dt \text{tr} V \partial_t V^\dagger \Lambda. \quad (3)$$

Here Λ is a diagonal matrix

$$\Lambda = \begin{pmatrix} \mathbb{1}_N & 0 \\ 0 & -\mathbb{1}_M \end{pmatrix} \quad (4)$$

and $\mathbb{1}_N$ and $\mathbb{1}_M$ denote $N \times N$ and $M \times M$ identity matrices, respectively. Assume that for $\varepsilon < 0$ the dangling spin is

located at the edge on the left ($j = 0$); then, for $\varepsilon > 0$ the single spin appears at the edge on the right ($j = L = 2N_s$). The complete effective action for the open spin chain in the large N limit now equals

$$S_{\text{open}} \rightarrow \mathcal{F}_0 + S_{\text{edge}}[V]. \quad (5)$$

Here $\mathcal{F}_0 = \beta E_0(\varepsilon)$ denotes the bulk free energy, β is the inverse temperature, and $S_{\text{edge}}[V]$ describes the critical theory of the edge,

$$S_{\text{edge}}[V] = i \frac{k(\varepsilon)}{2} \Omega[V(L)] + i \frac{1-k(\varepsilon)}{2} \Omega[V(0)], \quad (6)$$

with $k(\varepsilon) = \frac{1}{2}(1 + \frac{\varepsilon}{|\varepsilon|})$ the Heaviside step function.

A. Haldane mapping

Next, to make contact with the theory of the nonlinear sigma model we write

$$S_{\text{edge}}[V] = \frac{i}{2} \Omega[V(0)] + 2\pi i k(\varepsilon) \mathcal{C}[Q]. \quad (7)$$

Here $Q = V^\dagger \Lambda V \in \frac{U(N+M)}{U(N) \times U(M)}$ has a fractional topological charge $-\frac{1}{2} < \mathcal{C}[Q] \leq \frac{1}{2}$. Expressed as a two-dimensional space-time integral we can write [1–5]

$$\mathcal{C}[Q] = \frac{1}{16\pi i} \int d^2x \text{tr} \epsilon_{\mu\nu} Q \partial_\mu Q \partial_\nu Q, \quad (8)$$

with $\epsilon_{\mu\nu}$ the Levi-Civita symbol. This expression must be compared with the more general results of linear response theory. Similar to the dimer model, the purpose of the general theory is to formulate an effective action for the edge modes V or Q relative to a theory of bulk excitations. The latter always corresponds to a compact space-time geometry or, for that matter, a closed spin chain. Specifically, we must compare

$$2\pi i k(\varepsilon) \mathcal{C}[Q] \leftrightarrow \frac{\sigma_0}{8} \int d^2x \text{tr} (\partial_\mu Q)^2 + 2\pi i \sigma_H \mathcal{C}[Q]. \quad (9)$$

We know—from replica field theory of the electron gas—that the quantities $\sigma_0 = \sigma_0(\varepsilon; \beta, L)$ and $\sigma_H = \sigma_H(\varepsilon; \beta, L)$ precisely stand for the Kubo formulas for the macroscopic “longitudinal” and “Hall” conductance, respectively. Apparently the spin chain with $N \rightarrow \infty$ displays the QHE:

$$\sigma_0(\varepsilon; \beta, L) \leftrightarrow 0, \quad \sigma_H(\varepsilon; \beta, L) \leftrightarrow k(\varepsilon) \quad (10)$$

for all β and L . At the same time, one can probe the critical edge excitations more directly by measuring the local magnetization $\mathcal{M}_j \propto \text{tr}(\hat{S}_j \Lambda)$. Equation (6) implies

$$\mathcal{M}_{j=0} = \frac{1}{2}[1 - k(\varepsilon)], \quad \mathcal{M}_{j=2N_s} = \frac{1}{2}k(\varepsilon). \quad (11)$$

Notice that sum $\sum_j \mathcal{M}_j = \frac{1}{2}$ is a conserved quantity as it should be. Equation (11) now indicates that at criticality, a spin $\frac{1}{2}$ gets transported over macroscopic distances, from one edge of the spin chain to the other.

In conclusion, one can say that the dimer model provides a very simple but profound demonstration of the superuniversal features of the ϑ vacuum concept that are inaccessible otherwise.

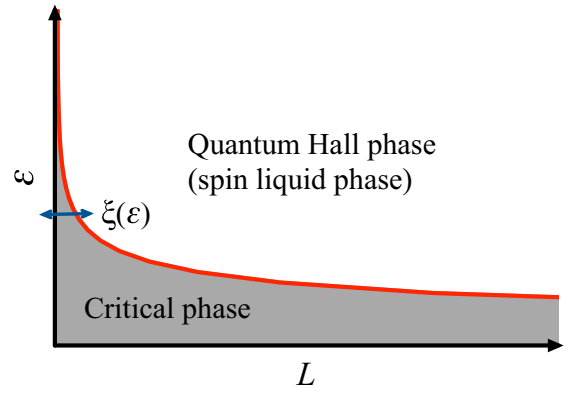


FIG. 2. Sketch of $|\varepsilon| = m(L)$ (solid red line) with $m(L)$ given by Eqs. (13) and (14). This line defines the correlation length $\xi(\varepsilon)$ which diverges continuously as $\varepsilon \rightarrow 0$, see text.

B. Instantons

Provided N, M and L are finite, one always finds that the discontinuity in Eqs. (2) and (10) gets smoothed out due to the tunneling events (instantons) between the two different dimer states. The situation is completely analogous to the recently revisited large N expansion of the CP^{N-1} model or $SU(N)/U(N-1)$ nonlinear sigma model [4]. In brief, the dimensionless ground state energy $\mathcal{E}_g = 2E_0(\varepsilon)/Le_2$ with $L = 2N_s$ the length of the spin chain, can in general be written as follows:

$$\mathcal{E}_g = -d - b\sqrt{\varepsilon^2 + m^2(L)}. \quad (12)$$

Here $b, d = 1 + \mathcal{O}(\frac{1}{N+M})$, whereas the function $m(L)$ is the most significant quantity. It has the general form

$$m(L) = L^{-\alpha_0} e^{-\beta_0 L - \gamma_0}, \quad (13)$$

with positive coefficients α_0, β_0 , and γ_0 given by

$$\alpha_0 = 1, \quad \beta_0 = \frac{(NM)^{3/2}}{2(N+M)^2}, \quad \gamma_0 = \frac{1}{2} \ln\left(\frac{NM}{4}\right). \quad (14)$$

C. “Phase” diagram

It is important to keep in mind that Eqs. (12) and (13) apply to *closed* spin chains without edges. Nevertheless, in what follows we will argue the instanton results explain most of the important features of *open* systems as well. For example, one might expect that the quantity $m(L)$ in Eq. (12) primarily affects the *critical regime* $|\varepsilon| \lesssim m(L)$ where the discontinuities in \mathcal{E}_g and σ_H are smoothed out. On the other hand, the effect of $m(L)$ is negligible or exponentially small in the *quantum Hall regime* $|\varepsilon| \gtrsim m(L)$ where Eq. (10) is likely to be valid. There are, in fact, two important conclusions that one can draw at this stage.

(1) The line $|\varepsilon| = m(L)$ represents the interface between the two distinctly different physical regimes in the problem, see Fig. 2. It is natural to identify the function

$$\xi(\varepsilon) = m^{-1}(\varepsilon) \quad (15)$$

as the *correlation length* in the problem. Remarkably, $\xi(\varepsilon)$ diverges in a continuous fashion as ε passes through zero.

(2) Exact expressions for the response parameters σ_0 and σ_H in Eq. (9) have been obtained based on the closely related large N steepest descend methodology of the CP^{N-1} model [4]. Specifically, one measures the response of the system to a change in boundary conditions (BC), namely in going from periodic BC in space-time to an open system or free BC. In this special case, the response can be very simply expressed in terms of ordinary derivatives of the ground state energy \mathcal{E}_g of the closed system (with periodic BC). Given the anisotropic space-time geometry at hand we now have $\sigma_{xx} \neq \sigma_{tt}$ and we can write

$$\begin{aligned} \sigma_{tt} &= 0, & \sigma_{xx} &= -m(L) \frac{\partial \mathcal{E}_g}{\partial m(L)} = \frac{m^2(L)}{\sqrt{\varepsilon^2 + m^2(L)}}, \\ \sigma_H &= \frac{1}{2} \left[1 - \frac{\partial \mathcal{E}_g}{\partial b\varepsilon} \right] = \frac{1}{2} \left[1 + \frac{\varepsilon}{\sqrt{\varepsilon^2 + m^2(L)}} \right]. \end{aligned} \quad (16)$$

III. NUMERICAL OBJECTIVES

Figure 2 and, in particular, Eq. (15) immediately reveal what happens to the “dangling edge spin” of the open chain as one approaches the critical point. For example, imagine that $L \geq 0$ in Fig. 2 actually stands for the position along a semi-infinite spin chain. Then it is natural to assume that for a given value of $\varepsilon > 0$ the phrase “critical phase” really means “massless chiral edge excitations” that are spread out over the region $0 \leq L < \xi(\varepsilon)$. So rather than being confined to the single lattice site at the edge ($L = 0$)—as naively expected on the basis on the large N result of Eq. (7)—the edge excitations are carried in practice by a whole range of spins and eventually, as ε approaches zero, by the entire spin chain. The divergent correlation length $\xi(\varepsilon)$ is therefore the *mechanism* that enables the dangling spin to travel over macroscopic distances, from one edge of the spin chain to the other, as ε passes through the critical point. In different words, the divergent length scale $\xi(\varepsilon)$ *unifies* the different types of quantum critical behavior in the problem, notably the quantum Hall plateau transition in $1 + 1$ space-time dimension that occurs for $\varepsilon = 0$ (or $\vartheta = \pi$) on the one hand, and the massless chiral edge excitations (dangling edge spins) that generally exist when $\varepsilon \neq 0$ (or $\vartheta \neq \pi$) on the other. These previously unrecognized features of the ϑ angle concept are quite remarkable, especially since they are expected to hold independent of the nature of the quantum phase transition at $\varepsilon = 0$ (or $\vartheta = \pi$). More specifically, the transition need not necessarily be a *second order* one; the aforementioned features are also displayed by systems—like the present ones—that undergo a *first order* transition.

Equally remarkable and important, however, is the fact that the diverging correlation length $\xi(\varepsilon)$ now manifests itself as a *directly observable* physical quantity of the system. This is so because the local magnetization of the ground state $\mathcal{M}_j(\varepsilon)$ is in fact a probe for the massless excitations that propagate along the edges. However, unlike the large N result of Eq. (11), one expects that $\mathcal{M}_j(\varepsilon)$ is now spread out over the entire range $0 \leq j < \xi(\varepsilon)$ rather than the single lattice site at $j = 0$ alone.

In what follows we embark on the numerical investigations of the physical scenarios discussed above in the context of dimerized spin chains.

IV. DMRG RESULTS AND DISCUSSION

Our numerical studies are based on the DMRG technique [12, 13]. Our main focus is on the ground state properties of the open dimerized $SU(N + M)$ spin chain with $S = \frac{1}{2}$ and an odd number of sites. We have used both infinite and finite system DMRG algorithms and constructed the superblock configuration with one exact site in the middle of adjacent blocks at each iteration. For each different set of N and M we use a different number (p) of the most probable eigenstates of the reduced density matrix. The DMRG calculations were done with $p \gtrsim 216$. In the finite system DMRG algorithm we have used eight to ten sweeps for convergence purposes. Our results are accurate up to density matrix truncation errors on the order of 10^{-7} . It should be mentioned that we are working with a single irreducible representation of $SU(N + M)$ characterized by the little group $U(N) \times U(M)$. This representation is the same as the Hilbert space of M fermions that can occupy $N + M$ states. We initially construct the basis with a definite number of fermions in each state. This defines the Cartan subgroup of $N + M - 1$ mutually commuting generators. The $SU(N + M)$ symmetric Hamiltonians we need to numerically diagonalize will hence be block diagonal in the different sectors of the quantum numbers. However, we have not kept track of these quantum numbers in our DMRG calculations.

A. Ground state energy

In Fig. 3 we plot the data for the dimensionless ground state energy \mathcal{E}_g versus ε ,

$$\mathcal{E}_g = E_0/N_s e_2, \quad (17)$$

where $e_2 = J \times NM(1 + \frac{1}{N+M})$ denotes the exact dimer energy for coupling strength J [10]. The results for different values of $(N, M) = (3, 1), (5, 1), (7, 1),$ and $(2, 2)$ and a range of values of $L = 4, 8, 14, 24, 34, 50,$ and 110 compare very well with the large N expression of Eq. (2). The main difference is the smoothening of the discontinuity at $\varepsilon = 0$ valid for all finite values of $N, M,$ and L . Moreover, for each given value of L , the data with increasing N clearly display a tendency toward the dimer model result $\mathcal{E}_g = -1 - |\varepsilon|$. Therefore, the main features of Fig. 3 are all in remarkable qualitative agreement with the instanton expressions of Eqs. (12) and (13).

To account for the fact that the DMRG data and the large N results of Eqs. (12)–(16) really belong to two different physical systems (open versus closed) we mention the following.

(1) *Critical phase.* The instanton expressions generally provide a good description of the numerical data in the critical phase $|\varepsilon| \lesssim m(L)$. Specifically, we obtain a good fit using Eqs. (12) and (13) with the coefficients b and d given by

$$b \sim 1 - \frac{b_1}{N + M}, \quad d \sim 1 + \frac{d_2}{(N + M)^2} \quad (18)$$

and with b_1 and d_2 positive constants. In addition to this, we find that the function of $m(L)$ in Eq. (13) applies to the DMRG data as well. Specifically, we employ the general expression $m(L) = L^{-\alpha_0} e^{-\beta_0 L + \gamma_0}$ with $\alpha_0, \beta_0,$ and γ_0 serving as N, M -dependent fitting parameters. It should be mentioned that any detailed comparison of the DMRG data with the

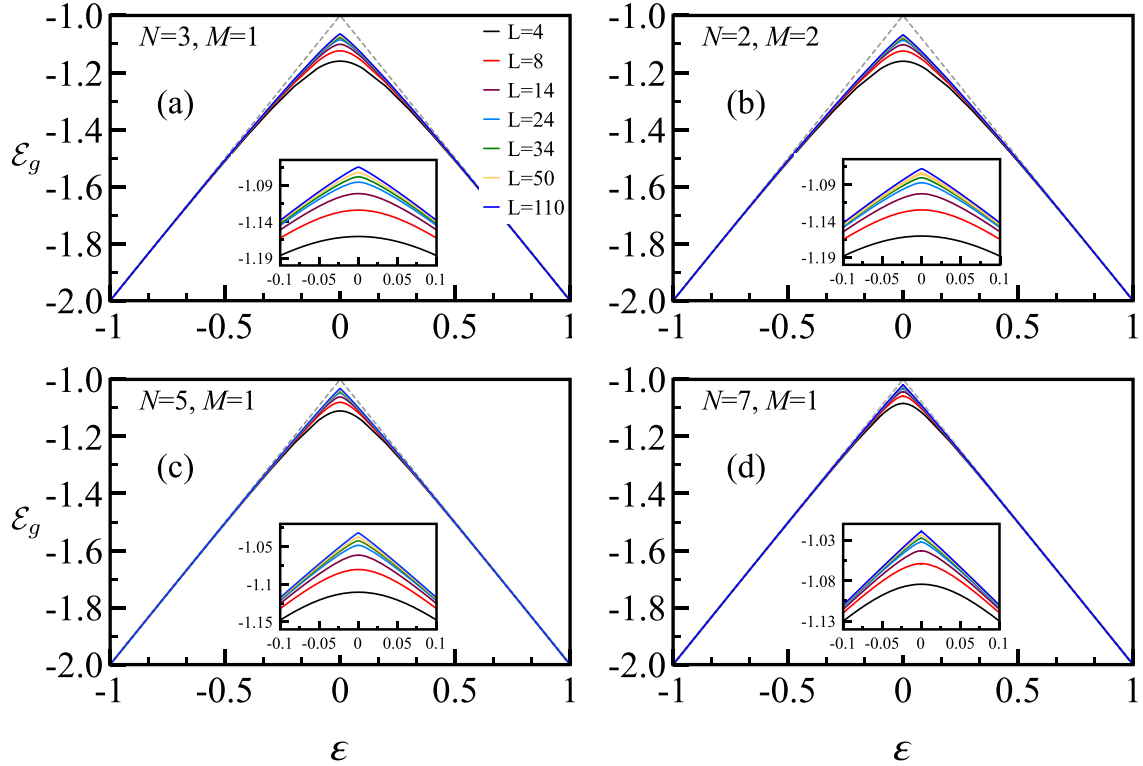


FIG. 3. DMRG results for the dimensionless ground state energy (\mathcal{E}_g) vs dimerization parameter (ϵ) for different N, M values and system sizes (L). The dashed lines represent the large N saddle point result of Eq. (2).

numerical values of Eq. (14) is moot. This is so because the physical mechanisms describing the function $m(L)$ are generally very different depending on whether one considers an open spin chain rather than closed systems.

(2) *Spin liquid phase.* Similar conclusions apply to the CP^{N-1} results for the conductances. For example, if one inserts the DMRG data for \mathcal{E}_g in Eq. (16), then one would naively conclude that the spin chain does not display the quantum Hall effect. The problem, of course, is that the subtle features of the edges are being mishandled since the \mathcal{E}_g in Eq. (16) is really defined for closed systems.

We now proceed and embark on the magnetic features of the open spin chain. Along the way we will find an alternative definition of the Hall conductance and obtain a better insight into the physical properties of both the critical and spin liquid phases of the problem.

B. Massless chiral edge excitations

To define the penetration of the edge excitations into the interior of the system, it is convenient to introduce the ‘‘cumulative’’ edge magnetization

$$\mathbf{P}(j) = \sum_{i=0}^j \mathcal{M}(i), \quad (19)$$

with $j \in \{0, 1, 2, \dots, 2N_s\}$ denoting the lattice site. Since the total magnetization is a conserved quantity, we use the normalization $\mathbf{P}(L) = \sum_{i=0}^L \mathcal{M}(i) = 1$ with $L = 2N_s$. In Fig. 4 we plot the numerical data for $[1 - \mathbf{P}(j)]$ versus j^2 on a log-

linear scale for different values of ϵ close to the critical point. Discarding the antiferromagnetic fluctuations in $\mathbf{P}(j)$ —which are relatively small—we have

$$\mathbf{P}(j) = 1 - A \exp\{-Bj^2\}, \quad (20)$$

with $A, B > 0$, provided L is large enough. It is clear that Eq. (20) really stands for the probability of finding the dangling edge spin somewhere in the region of the lattice sites between j and 0. Figure 4 clearly indicates that $B = B(\epsilon)$ generally decreases as ϵ goes to zero. It is therefore natural

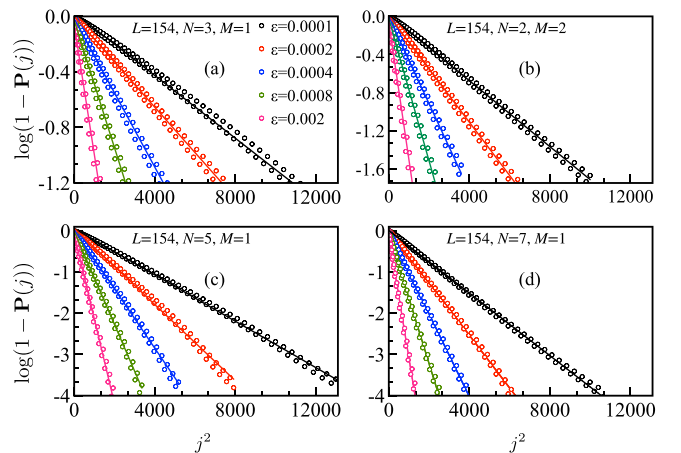


FIG. 4. DMRG data of $\log[1 - \mathbf{P}(j)]$ vs j^2 , see text. The solid lines represent the optimal fitting based on Eq. (20).

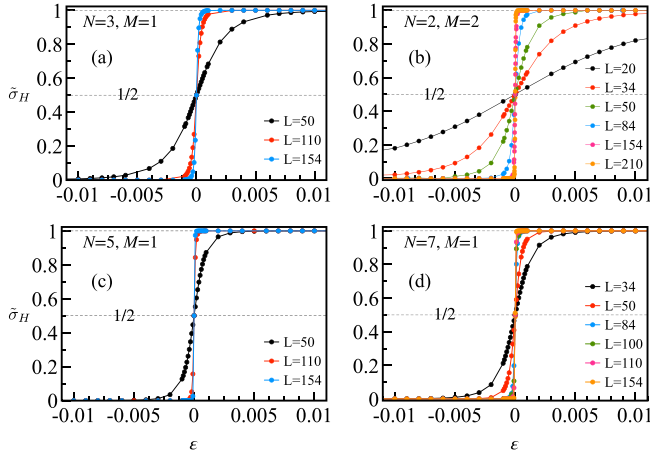


FIG. 5. DMRG results for the Hall conductance ($\tilde{\sigma}_H$) vs dimerization parameter (ε) for different N, M values and system sizes (L).

to identify the quantity $\xi(\varepsilon) = 1/\sqrt{B}$ as the continuously diverging *correlation length* of the system.

C. Hall conductance

A remarkable feature of open spin chains in the spin liquid phase $|\varepsilon| > m(L)$ is that the quantization of the Hall conductance is directly related to the conservation of total magnetization. This is obviously the case in the large N limit where $m(L) = 0$, see Eqs. (10) and (11), but the same is true in general. For example, from Eq. (20) we infer that $\sigma_H(\varepsilon) = 1 - \mathbf{P}(j)$ provided $\xi(\varepsilon) < j < L$. It is not difficult to generalize this statement to include the critical phase $|\varepsilon| < m(L)$ or $L > \xi(\varepsilon)$. Specifically, if we denote the magnetic definition of the Hall conductance by $\tilde{\sigma}_H(\varepsilon)$, then we can write

$$\tilde{\sigma}_H(\varepsilon) = 1 - \frac{1}{2}[\mathbf{P}(N_s) + \mathbf{P}(N_s - 1)], \quad (21)$$

which is nothing but the total magnetization of exactly the right half of the spin chain. Notice that duality of the spin chain $\varepsilon \leftrightarrow -\varepsilon$ implies that

$$\tilde{\sigma}_H(\varepsilon) = 1 - \tilde{\sigma}_H(-\varepsilon). \quad (22)$$

This fundamental symmetry, sometimes termed ‘‘particle-hole’’ symmetry, was originally predicted as a corollary of the renormalization theory of the quantum Hall effect [3]. It is clearly recognizable in the numerical data plotted in Figs. 5 and 6. These DMRG results are very similar to the plots obtained using the large N expression for σ_H , Eq. (16). In particular, Fig. 5 indicates that $\tilde{\sigma}_H$ with varying ε approaches the dimer result $k(\varepsilon)$ of Eq. (11) as N increases, keeping L fixed and finite. Therefore, just like the ground state energy \mathcal{E}_g we again find remarkable qualitative agreement with the instanton expression for $m(L)$ in Eq. (16).

Finally, it is interesting to notice that the numerical data of Fig. 5 and the flow lines of Fig. 6 are akin to the results of the first experiments on quantum criticality in the quantum Hall regime [40]. This illustrates the fact that superuniversality has a much broader range of validity than $SU(N + M)$ spin chains, the free electron gas ($N = M = 0$), and large N expansions alone. In fact, extensive research over many

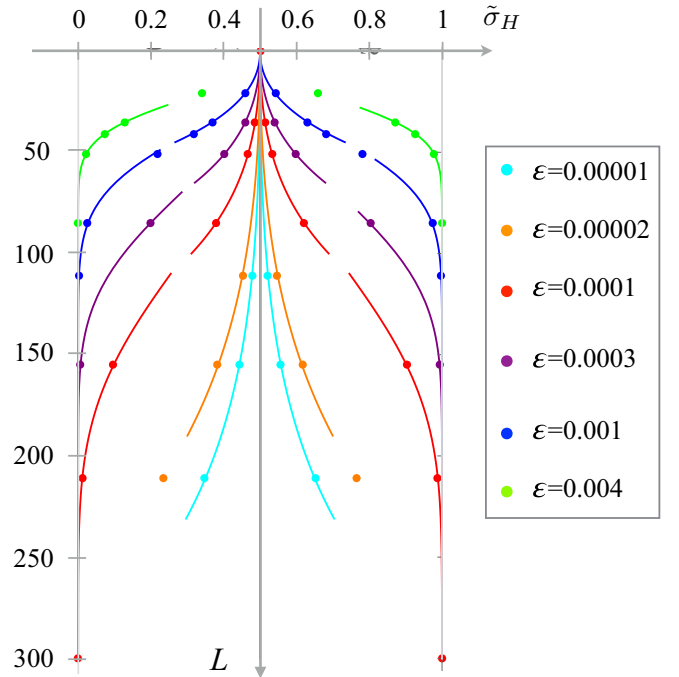


FIG. 6. DMRG results for the Hall conductance ($\tilde{\sigma}_H$) vs system size (L) for $N = M = 2$ and different values of the dimerization parameter (ε). The solid lines with $0.3 \lesssim \tilde{\sigma}_H \lesssim 0.7$ are the best fit based on the function $\tilde{\sigma}_H = \frac{1}{2} \pm \Gamma_1 \exp\{\beta_1 L + 2.1 \ln L\}$ with positive coefficients $\Gamma_1 \propto |\varepsilon|$ and β_1 . Those with $\tilde{\sigma}_H \lesssim 0.3$ and $\tilde{\sigma}_H \gtrsim 0.7$ have been obtained using $\tilde{\sigma}_H = \Gamma_2 \exp\{-\beta_2 L^2\}$ and $\tilde{\sigma}_H = 1 - \Gamma_2 \exp\{-\beta_2 L^2\}$, respectively, with positive Γ_2 and β_2 .

years has shown that the same basic phenomena are being displayed by entirely different physical systems. The most obvious examples include the electron gas in the presence of the Coulomb interaction [4,18] and also the problem of ‘‘macroscopic charge quantization’’ in the single electron transistor [41,42].

D. Singularity structure open chains

Of principal interest are three distinctly different functions $F(X)$ that diverge continuously as X goes to infinity.

(i) The first and most significant of these is the second derivative of the ground state energy \mathcal{E}_g at the critical point

$$F_{\text{Energy}}(L) = \left. \frac{\partial^2 \mathcal{E}_g}{\partial \varepsilon^2} \right|_{\varepsilon \rightarrow 0} \leftrightarrow \frac{1}{m(L)}. \quad (23)$$

The quantity $1/m(L)$ on the right-hand side indicates the instanton result of Eqs. (13) and (14) for the closed spin system with varying size L . We therefore expect that the DMRG data for $F_{\text{Energy}}(L)$ diverge exponentially as L increases. An explicit demonstration of this divergence can be taken as the experimental proof of a first order quantum phase transition at $\varepsilon = 0$ (or $\theta_B = \pi$). The most practical way of extracting Eq. (23) from DMRG is to first compute $\partial \mathcal{E}_g / \partial \varepsilon$ for a discrete set of ε values and subsequently determine the second derivative using the standard numerical programs. For the purpose of the present paper, it suffices to fix the spacing $\Delta \varepsilon$ at 10^{-5} .

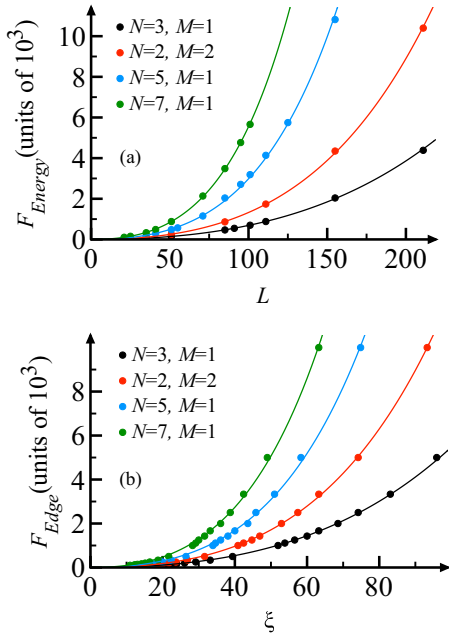


FIG. 7. DMRG results for the functions $F_{\text{Energy}}(L)$ and $F_{\text{Edge}}(\xi)$ for different N, M values, see text. The solid lines are optimal fittings based on Eqs. (26) and (28).

In Fig. 7(a) we plot the DMRG data sets for four different values of N and M .

(ii) The second most significant quantity is the correlation length ξ with varying ε . We have seen that unlike Eq. (23), the ξ is solely defined as a quantity of the edge. As a practical rule we demand that ξ for any given value of ε is determined by the equation $\mathbf{P}(j = \xi) = 1 - e^{-1.5} \approx 0.78\%$ where $\mathbf{P}(j)$ is defined by Eq. (19). In words, there is a 78% probability of finding a dangling spin somewhere in the region of lattice sites $0 \leq j \leq \xi$.

In Fig. 7(b) we plot $1/\varepsilon$ versus the DMRG data for ξ for the aforementioned values of N and M . The different data sets provide and estimate for the function $F_{\text{Edge}}(\xi)$, i.e.,

$$F_{\text{Edge}}(\xi) = \frac{1}{\varepsilon} \leftrightarrow \frac{1}{m(\xi)}, \quad (24)$$

where the right-hand side is the result of the large N theory, see Eq. (15). Indeed, the plots of Figs. 7(a) and 7(b) clearly indicate that the functions $F_{\text{Energy}}(L)$ and $F_{\text{Edge}}(\xi)$ display the same qualitative features for varying values of N and M .

(iii) From the physics point of view, our main interest is obviously in the singularity structure of the quantum Hall plateau transition described by the function

$$F_{\text{Hall}}(L) = \left. \frac{\partial \tilde{\sigma}_H}{\partial \varepsilon} \right|_{\varepsilon \rightarrow 0} \leftrightarrow \frac{1}{m(L)}, \quad (25)$$

with $\tilde{\sigma}_H$ defined by Eq. (21). Just like Eq. (23), the most practical way of extracting Eq. (25) from DMRG is to compute $\tilde{\sigma}_H$ for a discrete set of ε values and subsequently determine the derivative using the standard numerical programs.

In a subsequent paper we will show that the large N limit of Eq. (25), like Eq. (23), is $1/m(L)$ [10]. For comparison we plot, in Fig. 8, the DMRG data sets for the three different functions $F_{\text{Energy}}(L)$, $F_{\text{Edge}}(\xi)$, and $F_{\text{Hall}}(L)$, taking the case

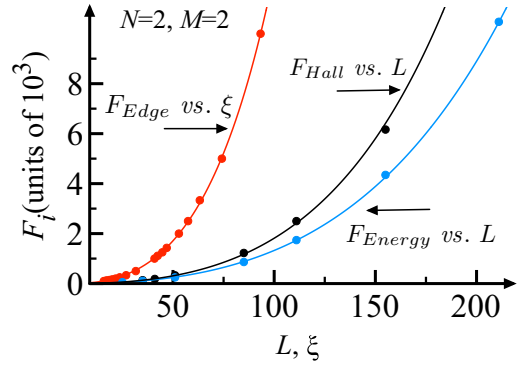


FIG. 8. DMRG results for the functions $F_{\text{Hall}}(L)$, $F_{\text{Energy}}(L)$, and $F_{\text{Edge}}(\xi)$ with $N = M = 2$, see text. The solid lines are optimal fittings based on Eqs. (26) and (28).

$N = M = 2$ as a representative example. Once more, apart from a simple rescaling of the X and/or Y axis, the results look qualitatively very similar.

E. Universality revealed

To find the best solid lines through the data in both Figs. 7 and 8 we are inspired by instanton results of Eqs. (13) and (14). Specifically, we write

$$F_i(X) = a_i F(b_i X), \quad (26)$$

where the subscript i stands for Energy, Edge, and Hall, respectively. The coefficients a_i and b_i are taken as independent fitting parameters and $F(X)$ is an empirical function without free parameters. To fix the thought consider the large N limit with $F_i(X) = 1/m(X)$. We can write $F(X) = X \exp\{X\}$ in Eq. (26) and

$$a_i \rightarrow \frac{N}{M}, \quad b_i \rightarrow \frac{1}{2} M \sqrt{\frac{N}{M}} \quad (27)$$

keeping in mind that $N \rightarrow \infty$ and M is fixed and finite. Notice that Eq. (27) implies that $F_i(X)$ increases as the value of N increases. This feature is in accordance with the DMRG data plotted in Figs. 7(a) and 7(b).

The problem, however, is to find an optimal function $F(X)$ such that Eq. (26) can be used for data fitting for all values of N and M as well as the subscript i . After a lot of trial and error we found the best function $F(X)$ in Eq. (26) to be $F(X) = X^{2.1} \exp\{X\}$. We will work with the completely equivalent but more practical expression

$$F(X) = X^{2.1} \exp \left\{ -2.5 + \frac{X}{150} \right\}, \quad (28)$$

which corresponds, roughly speaking, to the ‘‘average’’ of the nine different DMRG data sets.

The solid lines in both Figs. 7 and 8 clearly show that Eqs. (26) and (28) fit the DMRG data remarkably well. The most important feature of these expressions, however, is that each of the nine DMRG data sets can be mapped onto the single curve $Y = F(X)$ after a simple rescaling of the X and Y axes. This data collapse is plotted in Fig. 9. We see that the rescaled DMRG data all fall nicely onto the solid line $F(X)$, as expected.

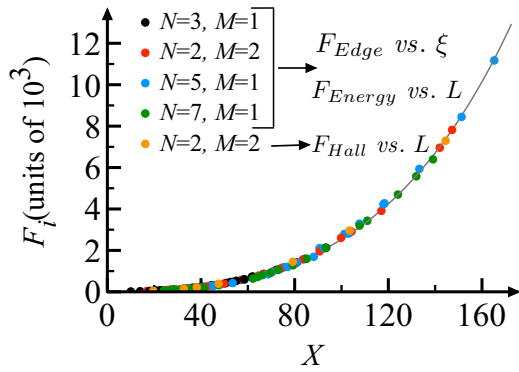


FIG. 9. Collapse of the nine different data sets of Figs. 7 and 8 after rescaling. The solid line represents the function $F(X)$, Eq. (28), with $X = L$ or ξ .

V. CONCLUSION

The principal advancement of this paper is captured in Fig. 9. The DMRG data clearly indicate that the basic predictions of the large N theory can be trusted all the way down to the regime where $N + M$ is of order unity. The results furthermore unify the general features of a first order phase transition with quantum phenomena that were previously unrecognized. We mention, in particular, the *robustly* quantized Hall plateaus along with the *deconfinement* mechanism that facilitates the transport of a dangling spin (or massless edge excitations) over macroscopic distances [9,14]. This mechanism can be depicted as a spatial separation between the critical phase and the spin liquid phase (see Fig. 2).

We have refined and extended the concept of superuniversality to include the correlation length ξ that diverges continuously as one approaches the critical point. As a result, we can now say that the basic aspects of quantum Hall physics are all generic topological features of the ϑ vacuum concept on the strong coupling side, for all non-negative values of N and M [1–4].

It should be mentioned that the space-time geometry of the spin chain is somewhat unnatural, at least as far as the QHE is concerned. The quasi-one-dimensional geometry with $\beta \rightarrow \infty$ and L finite is clearly very different from the truly

two-dimensional quantum Hall system which usually involves $\beta \sim L$. Without going into further detail, however, we can say that as an integral aspect of the superuniversality concept one expects that the basic phenomena are independent of the geometry that one considers. For example, based on the large N theory of the CP^{N-1} model [4] we know that the differences are solely in the detailed behavior of the function $F(X)$. Unlike Eq. (28) this function is algebraic for systems where β and L play a role of equal significance. Specifically,

$$F(X) \propto X^{1/\nu}, \quad (29)$$

where X stands for either $L \sim \beta$ or ξ . The ν denotes the correlation length exponent which for the systems at hand is equal to $1/2$, a well known result for a first order transition in two dimensions.

Equation (29) is an extremely familiar statement that is valid for both first and second order quantum phase transitions. However, as one of the interesting new features of the ϑ vacuum—and along with that, the quantum Hall plateau transition—we now find that the correlation length ξ *always diverges* in a continuous manner as ϑ approaches π . Moreover, the physical quantity ξ is *directly measurable* and manifests itself most clearly as a kind of penetration depth of the massless chiral edge excitations.

Finally, the precise correspondence between the bulk excitations and those at the edges of the spin chain has been actually established by the function $F(X)$ as discovered in this paper. This remarkable topological aspect is not seen in the theory of ordinary critical phenomena.

ACKNOWLEDGMENTS

The authors gratefully acknowledge the HPC Nandadevi cluster at the Institute of Mathematical Sciences (IMSc, Chennai) for providing computational facilities. A.M.M.P. is indebted to the IMSc for visiting appointments. B.D. acknowledges the Würzburg-Dresden Cluster of Excellence on Complexity and Topology in Quantum Matter - ct.qmat, the Swiss National Science Foundation and the IMSc for financial support. B.D. also thanks Fakher F. Assaad, Frederic Mila and R. Ganesh for stimulating discussions and their support for this project.

-
- [1] H. Levine, S. B. Libby, and A. M. M. Pruisken, *Phys. Rev. Lett.* **51**, 1915 (1983).
 - [2] H. Levine, S. B. Libby, and A. M. M. Pruisken, *Nucl. Phys. B* **240**, 71 (1984).
 - [3] A. M. M. Pruisken, *The Quantum Hall Effect* (Springer, New York, 1990), Chap. 5.
 - [4] A. M. M. Pruisken, *Int. J. Mod. Phys. B* **24**, 1895 (2010).
 - [5] A. M. M. Pruisken, *50 Years of Anderson Localization* (World Scientific, Singapore, 2010), Chap. 21.
 - [6] F. D. M. Haldane, *Phys. Lett. A* **93**, 464 (1983).
 - [7] F. D. M. Haldane, *Phys. Rev. Lett.* **50**, 1153 (1983).
 - [8] I. Affleck, *Phys. Rev. Lett.* **54**, 966 (1985).
 - [9] A. M. M. Pruisken, R. Shankar, and N. Surendran, *Europhys. Lett.* **82**, 47005 (2008).
 - [10] A. M. M. Pruisken, B. Danu, and R. Shankar (in preparation).
 - [11] E. Brézin, S. Hikami, and J. Zinn-Justin, *Nucl. Phys. B* **165**, 528 (1980).
 - [12] S. R. White, *Phys. Rev. B* **48**, 10345 (1993).
 - [13] U. Schollwöck, *Rev. Mod. Phys.* **77**, 259 (2005).
 - [14] A. M. M. Pruisken, R. Shankar, and N. Surendran, *Phys. Rev. B* **72**, 035329 (2005).
 - [15] A. M. M. Pruisken, *Int. J. Theor. Phys.* **48**, 1736 (2009).
 - [16] A. M. M. Pruisken, B. Škorić, and M. A. Baranov, *Phys. Rev. B* **60**, 16838 (1999).
 - [17] B. Škorić and A. M. M. Pruisken, *Nucl. Phys. B* **559**, 637 (1999).
 - [18] A. M. M. Pruisken and I. S. Burmistrov, *Ann. Phys.* **322**, 1265 (2007).

- [19] A. D’Adda, M. Lüscher, and P. Di Vecchia, *Nucl. Phys. B* **146**, 63 (1978).
- [20] E. Witten, *Nucl. Phys. B* **149**, 285 (1979).
- [21] S. Coleman, *Ann. Phys.* **101**, 239 (1976).
- [22] I. Affleck, *Nucl. Phys. B* **162**, 461 (1980).
- [23] I. Affleck, *Nucl. Phys. B* **171**, 420 (1980).
- [24] C. G. Callan, R. F. Dashen, and D. J. Gross, *Phys. Rev. D* **20**, 3279 (1979).
- [25] R. Rajaraman, *Solitons and Instantons* (Elsevier, North Holland, 1987).
- [26] A. Polyakov, *Gauge Fields and Strings* (Harwood Academic, Chur, Switzerland, 1987).
- [27] A. Jevicki, *Phys. Rev. D* **20**, 3331 (1979).
- [28] S. Coleman, *Aspects of Symmetry* (Cambridge University Press, Cambridge, 1985).
- [29] I. Affleck, *Nucl. Phys. B* **257**, 397 (1985).
- [30] I. Affleck, *Nucl. Phys. B* **305**, 582 (1988).
- [31] I. Affleck, *Phys. Rev. Lett.* **66**, 2429 (1991).
- [32] J. J. M. Verbaarschot and M. R. Zirnbauer, *J. Phys. A: Math. Gen.* **18**, 1093 (1985).
- [33] M. Zirnbauer, *Ann. Phys.* **506**, 513 (1994).
- [34] M. Zirnbauer, *J. Math. Phys.* **38**, 2007 (1997).
- [35] I. Affleck and J. B. Marston, *Phys. Rev. B* **37**, 3774 (1988).
- [36] N. Read and S. Sachdev, *Nucl. Phys. B* **316**, 609 (1989).
- [37] A. M. M. Pruisken, M. A. Baranov, and B. Škorić, *Phys. Rev. B* **60**, 16807 (1999).
- [38] M. A. Baranov, A. M. M. Pruisken, and B. Škorić, *Phys. Rev. B* **60**, 16821 (1999).
- [39] A. M. M. Pruisken and I. S. Burmistrov, *Ann. Phys.* **316**, 285 (2005).
- [40] H. P. Wei, D. C. Tsui, and A. M. M. Pruisken, *Phys. Rev. B* **33**, 1488 (1986).
- [41] I. S. Burmistrov and A. M. M. Pruisken, *Phys. Rev. Lett.* **101**, 056801 (2008).
- [42] I. S. Burmistrov and A. M. M. Pruisken, *Phys. Rev. B* **81**, 085428 (2010).